

SMALL SCALE INTERACTIONS
IN THE
NEAR SURFACE OCEAN

Mark Christopher Haley

Library
Naval Postgraduate School
Monterey, California 93940

NAVAL POSTGRADUATE SCHOOL

Monterey, California



THESIS

SMALL SCALE INTERACTIONS
IN THE
NEAR SURFACE OCEAN

by

Mark Christopher Haley

Thesis Advisor:

E. B. Thornton

December 1972

715 000
Approved for public release; distribution unlimited.

Small Scale Interactions
in the
Near Surface Ocean

by

Mark Christopher Haley
Lieutenant, United States Navy
B. S., United States Naval Academy, 1967

Submitted in partial fulfillment of the
requirements for the degree of

MASTER OF SCIENCE IN OCEANOGRAPHY

from the
NAVAL POSTGRADUATE SCHOOL
December 1972

ABSTRACT

Experiments were conducted at the NURDC oceanographic tower off San Diego, California to describe the small scale physical properties in the upper ocean and to determine their temporal and spatial interrelationships. The measured parameters included water particle velocities, temperatures, salinity, sound speed, sound speed (phase) modulation, sound amplitude modulation and surface waves. Simultaneous time series measurements are analyzed for a twenty minute record taken at a depth of 7.3 m. The spatial correlation distance for temperature was found to be about 25 cm. Sound modulation of a 60 kHz sound beam underwent a mean attenuation of about 5%. The correlation distance of an effective inhomogeneity due to the combined temperature, salinity, and bubble effects was found to be 8.8 cm. The change in the index of refraction of the speed of sound at 60 kHz (a bubble resonant region) was found to be 99% induced by bubbles. The energy density spectra were dominated by wave induced motion. First order wave theory accurately predicts orbital water particle motion and its irrotationality. High coherence is found between wave-induced water particle motion and sound modulation and decreasing coherence between water particle motion and salinity, sound velocity, and temperature.

TABLE OF CONTENTS

I.	INTRODUCTION - - - - -	9
A.	BACKGROUND - - - - -	9
B.	RESEARCH OBJECTIVES - - - - -	10
II.	EXPERIMENT - - - - -	11
III.	INSTRUMENTATION - - - - -	17
A.	SOUND VELOCITY METER - - - - -	17
B.	THERMISTORS - - - - -	17
C.	WAVE HEIGHT METER - - - - -	17
D.	WATER CURRENT METER - - - - -	18
E.	SALINOMETER - - - - -	18
F.	SOUND AMPLITUDE MODULATION - - - - -	18
G.	SOUND VELOCITY (PHASE) - - - - -	19
IV.	DATA PRE-PROCESSING - - - - -	20
V.	ANALYSIS OF DATA - - - - -	22
A.	HIGH PASS FOURIER FILTER - - - - -	22
B.	SPECTRAL ANALYSIS - - - - -	24
C.	CONVERSION OF THE TIME SERIES MEASUREMENTS TO SPATIAL CORRELATIONS - - - - -	26
D.	CORRELATION DISTANCES AND DISTRIBUTION FUNCTIONS FOR TEMPERATURE - - - - -	28
E.	APPLICATION OF WILSON'S EQUATION - - - - -	34
F.	AMPLITUDE MODULATION IN A RANDOM MEDIUM - - - - -	38
	1. Establishing an "Effective" Correlation Distance - - -	38
	2. The Importance of Bubbles in the Near Surface Region -	41
G.	SURFACE WAVE EFFECTS OF THE ENERGY DENSITY, PHASE, AND COHERENCE SPECTRA OF ALL PARAMETERS - - - - -	45

VI. CONCLUSIONS	- - - - -	51
BIBLIOGRAPHY	- - - - -	53
INITIAL DISTRIBUTION LIST	- - - - -	54
FORM DD 1473	- - - - -	56

LIST OF TABLES

Table I	Calibration Factors for Data
Table II	Variances of Sound Velocity, Temperature, and Salinity

LIST OF FIGURES

- Figure 1 NURDC Oceanographic Research Tower
- Figure 2 Research Tower Schematic
- Figure 3 Spatial Configuration of Instruments
- Figure 4 Geometrical Separations Between Instruments
- Figure 5 Filtered and Unfiltered Temperature 2 Spectra
- Figure 6 Spatial Temperature Auto-correlation Functions
- Figure 7 Time Temperature Auto-correlation Functions
- Figure 8 Temperature 2 Probability Density Function Without
Fourier Filter
- Figure 9 Temperature 2 Probability Density Function With
Fourier Filter
- Figure 10 Wave Height and Temperature 2 Spectra
- Figure 11 Wave Height and Salinity Spectra
- Figure 12 Wave Height and Sound Modulation Spectra
- Figure 13 u and w Velocity Component Spectra
- Figure 14 Measured and Theoretical Vertical Velocities
- Figure 15 Wave Height and Sound Velocity Spectra

LIST OF SYMBOLS

A_n	Fourier Series Coefficient
a	Radius of Scattering Inhomogeneity in Meters
α	RMS Refractive Index Variation from Unity
B_n	Fourier Series Coefficient
b	Range from Source to Receiver
c	Speed of Sound in Meters per Second
$C_{12}(f)$	Co-spectrum
cov	Covariance
(cv)	Coefficient of Variation
$\mathcal{E}_{12}(f)$	Phase Angle
F	General Parameter
f	Frequency
$\gamma_{12}^2(f)$	Coherence Function
h	Depth from Surface to Bottom of Ocean in Meters .
k	Wave Number
$n(\omega)$	n th Harmonic of Fundamental Frequency ω
η	Wave Height in Meters
$\phi_{11}(\tau)$	Auto-covariance Function
$\phi_{12}(\tau)$	Cross-covariance Function
$\bar{\epsilon}_{11}(f)$	Energy Density Spectrum
$\bar{\epsilon}_{12}(f)$	Cross Density Spectrum
P	Pressure in Newtons per Meter ²
$\mathcal{P}(\tau)$	Parzen Window-Function
ρ	Lag Distance in Meters
$Q_{12}(f)$	Quadrature Spectrum

r	Length in Meters
s	Salinity in Parts per Thousand
T	Temperature in Degrees Centigrade
t	Time in Seconds
τ	Lag Time in Seconds
U	Velocity in Meters per Second
u	Horizontal Velocity Component in Meters per Second
μ	Index of Refraction of Speed of Sound
var	Variance
w	Vertical Velocity Component in Meters per Second
z	Depth in Meters

I. INTRODUCTION

A. BACKGROUND

The importance of detailed studies of sound propagation in the upper layer of the ocean has become increasingly apparent as the role of the submarine continues to grow in strategic and offensive capabilities. Also significant from a scientific viewpoint is that the manner in which sound propagates can be used to effectively describe properties of the medium. Thus in order to understand sound propagation, a detailed knowledge of the parameters that affect it and their interrelationships with each other and sound is required. Wilson [10] developed an equation that related the speed of sound in water to temperature, salinity, and pressure. Liebermann [4] delved into the effects of temperature inhomogeneities on sound propagation and determined that inhomogeneities do have an effect on the intensity and refraction of propagated sound waves. Mintzer and Stone [6] theoretically developed an equation that related to the reduction in sound intensity of a propagated wave to wave number, correlation distance, distance traveled and changes in the refractive index of the medium.

In November of 1971, Bordy [2], Duchock [3], Rautmann [7], Seymour [8], and Smith [9] from the Naval Postgraduate School took measurements at the NURDC tower of various oceanographic parameters in the near surface zone while propagating sound waves over prescribed paths. The parameters measured included sound velocity, sound amplitude and phase modulation, water particle velocities, temperature, salinity, and wave height. The main purpose of this paper is to extend the results of the references just cited carrying out a more detailed study of these parameters and their interrelationships.

B. OBJECTIVES

1. To determine the interrelationships between the various parameters (temperature, salinity, sound velocity, modulation and wave height) in the near surface ocean zone. Only those processes with periodicity between 0.5 to 50 seconds will be considered.
2. To compare results with established equations and relationships.

II. EXPERIMENT

On 21 October 1971, Bordy, Duchock, Rautmann, Seymour, and Smith from the Naval Postgraduate School conducted experiments at the Naval Undersea Research and Development Center Oceanographic Research Tower at San Diego, California. The purpose of the experiment was to describe the small scale physical properties in the upper ocean and to determine their temporal and spatial interrelationships. The tower is approximately one mile off Mission Beach in a mean water depth of 17 meters. The structure is made of steel and concrete and built into the sea floor. An enclosed upper deck provides space for electronic equipment while an open lower deck provides a platform to place instruments in the water. On the northern, southern, and western sides are located winch controlled instrument carriages that can be adjusted to any desired depth. (Figure 1 and Figure 2).

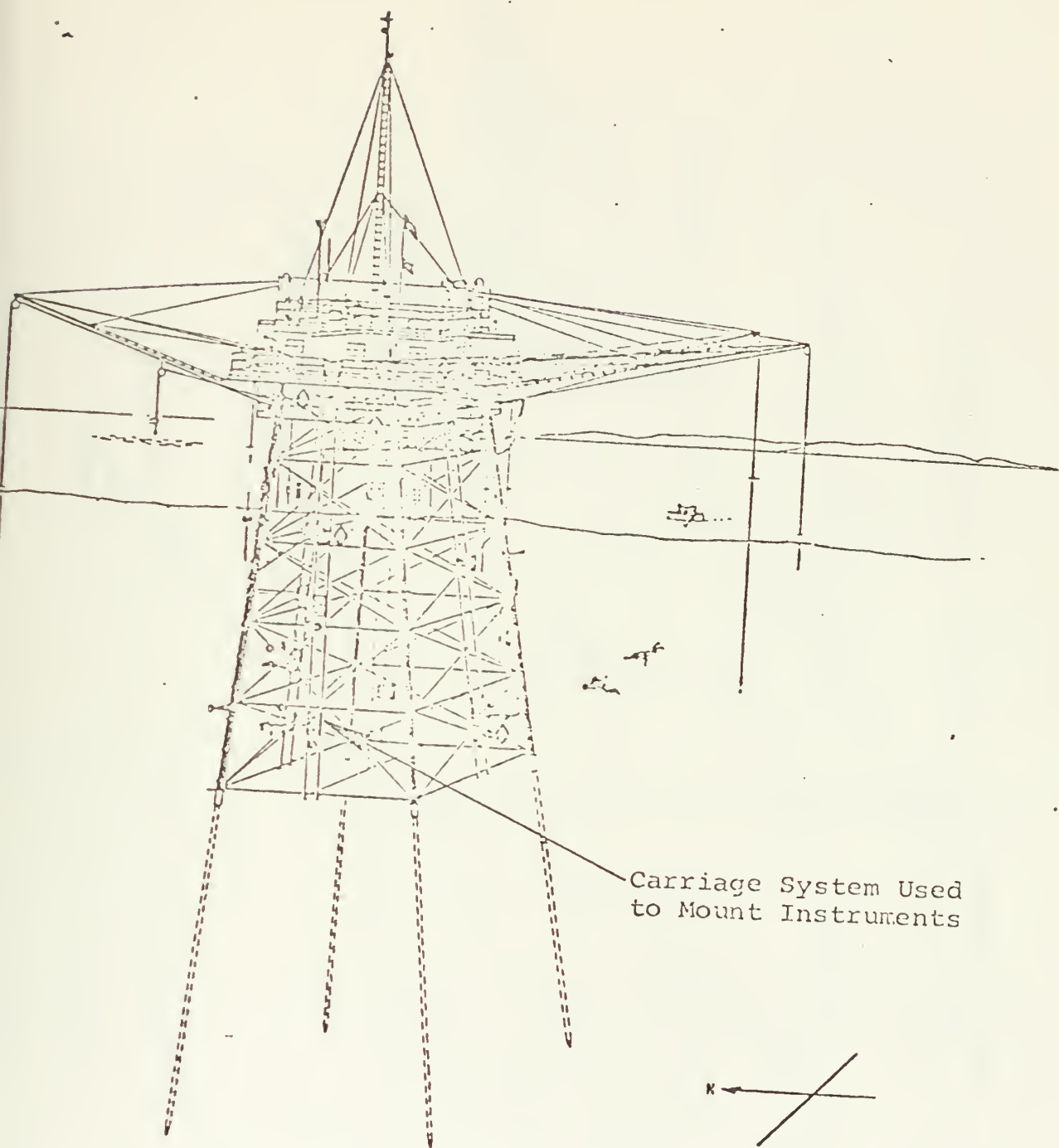
The parameters measured during the experiment included orthogonal water particle velocities, an array of temperatures, salinity, sound speed, sound speed (phase) modulations, sound amplitude modulation and surface waves measured directly over the column of interest. All sensors were placed within a 2 meter cube of water. Simultaneous time series measurements were made for twenty-minute durations. The experiments were conducted at four depths. In this paper, Run Five, at a depth of 7.3 meters, will be analyzed in detail. The spatial configuration of the sensors is shown in Figure 3. The actual geometrical separations are shown in Figure 4.

During the 24 hour period of the experiment, a bi-modal surface swell of about 0.3 meters height was visually observed with one component



Navy Undersea Research and Development Center
Oceanographic Research Tower

Figure 1.



Research Tower Schematic

Figure 2.

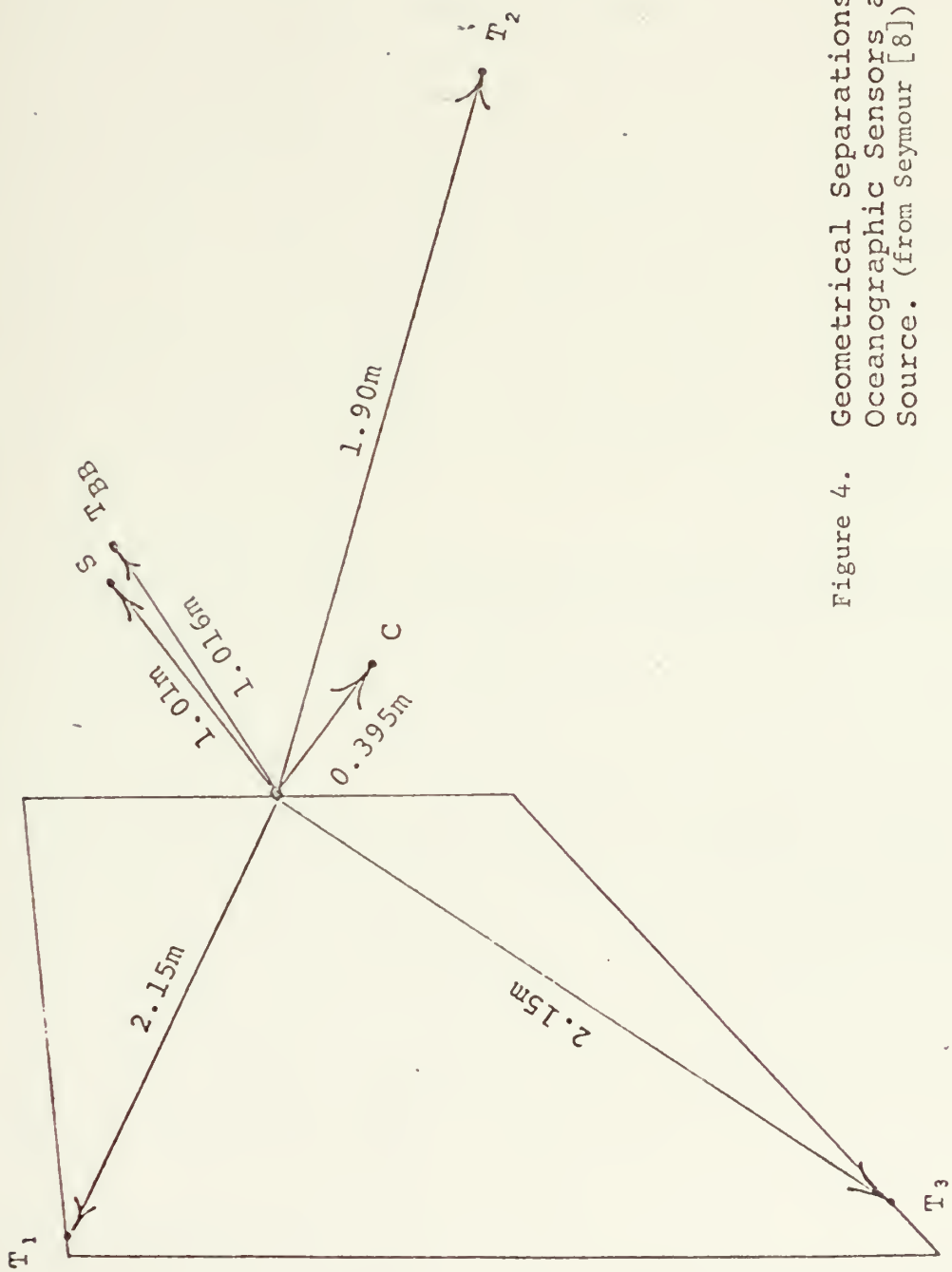


Figure 4. Geometrical Separations Between Oceanographic Sensors and Acoustic Source. (from Seymour [8]).

having a period of about 7 seconds from 285° true and the other component with a period of about 5 seconds from 260° true. The surface was observed to be non-breaking with a wind capillary system present. The wind was from 310° true at a speed of about 8 knots. A moderate temperature gradient was present with a temperature of 17.5° C at the surface decreasing to 15° C at a depth of 18 meters.

III. INSTRUMENTATION

A brief description of the instruments used will be given in this section. A more detailed description can be found in the papers of Bordy, Smith, Duchock, Rautmann, and Seymour. Instrument details are given in manufacturers' technical manuals.

A. SOUND VELOCITY SENSOR

Sound velocity was measured with a Ramsay MK-1 deep sea probe utilizing only the sound velocimeter portion of the probe. The Ramsay velocimeter is of the "sing-around" type consisting of a transducer and transmitter which transmits a pulse of 4 MHz into a 25 centimeter sound path. The pulse is reflected twice to reduce errors due to water motion.

B. TEMPERATURE SENSOR

Temperature was measured using a specially constructed Wheatstone bridge circuit utilizing a temperature sensitive thermistor as one leg of the circuit. For Run Five, two such circuits were employed. The type of temperature sensor used was a type K 496 isocurve thermistor manufactured by Fenwall Electronics, Inc., Farmington, Massachusetts. The specific thermistors were extracted from an expendable bathythermograph. It is a double-bead thermistor which incorporates a special aging process, giving stable and repeatable accuracies not usually obtained with ordinary thermistors. These thermistors have a time constant of 150 milliseconds.

C. BAYLOR WAVE GAUGE

The Baylor Model 13528 is a wave profile recording system which measures instantaneous sea surface elevation as a function of time.

Measurements are accurate within one percent of actual height. The system consists of three components: the wave staff, transducer and recorder. The transducer unit measures the electrical resistance of the length of the staff above the water surface. The conducting seawater provides a short circuit across the cables (wave staff) immersed in the water. A direct current voltage proportional to the height of the sea surface is taken across the resulting fluctuating resistance.

D. WATER CURRENT METER

The water particle velocities were measured with an Engineering Physics Company water current meter Model EMCM-3B. The EMCM-3B is an electromagnetic current measuring device that measures two orthogonal components of water particle velocity from zero to five meters per second. Two d.c. voltage signals proportional to the magnitude of the orthogonal velocity components are produced. The measured response is flat to at least 0.5 seconds, the high frequency limit of the calibration facility. The maximum output error is one percent of full scale reading.

E. SALINITY SENSOR

The salinity sensor employed was part of the Bissett-Berman STD Model 9006. An inductively-coupled sensor detects conductivity, which is also compensated for temperature and pressure effects, thereby producing an output totally dependent upon salinity. The time constant for the salinity sensor is .35 seconds.

F. MODULATION

In order to measure environmentally caused amplitude modulation in the ocean, a high frequency acoustic carrier wave was directed at a

receiving hydrophone mounted along the acoustic axis at a separation of two meters. An envelope detection system was used to measure the amplitude modulation of the received signal. A USRD type F-27 transducer and an Atlantic Research Corporation type LC-10 hydrophone were used in the experiments.

G. SOUND VELOCITY (PHASE)

In determining sound velocity by phase measurements, one F-27 transducer was used along with one LC-10 and one LC-5 hydrophone. See Rautmann [7] for further details.

IV. DATA PRE-PROCESSING

Run Five was started at 1728 and ended at 1748 on 21 October 1972. During the run, data was recorded on a Sangamo Model 3500, 14 channel FM tape recorder. The data consisted of temperatures 1 and 2, salinity, wave height, u and w water particle velocity components, sound modulation, and sound velocity. The taped data was transcribed to a rectangular eight channel Clevite Brush Recorder after amplification by Krohn-Hite Model 3322 variable filters.

A Calma Company Model 480 mechanical digitizer was used to digitize the continuous strip chart information at 100 points to the inch. This corresponds to a sampling interval of 0.2032 seconds. This information was recorded onto a 7 track magnetic tape which is compatible with the CDC 6500 computer at the Fleet Numerical Weather Central, Monterey. The data was transferred to cards using program CONVERT (Lynch, 1970) so that it could be read for analysis by the IBM 360 at the Naval Postgraduate School which uses 9 track magnetic tapes. The calibration factors used to convert the data into the appropriate units are listed in Table I.

TABLE I
CALIBRATION FACTORS FOR DATA

CALIBRATION FACTOR	MEASUREMENT	UNITS
.23	Temperature	$^{\circ}\text{C}$
.508	Salinity	ppt
.58	u, w	meters/second
.34	Sound Velocity	meters/second
.211	Fractional Modulation	
.775	Wave Height	meters

This information is included here to facilitate future analysis of this data.

V. ANALYSIS OF DATA

A. FOURIER FILTER

The experiment was designed to study processes in the approximate frequency band 0.02 to 2 Hz corresponding to time scales of 0.5 seconds to 50 seconds. The initial analysis of the raw data showed that the energy density spectra of some parameters had excessive leakage from the very low frequencies. The time correlations were of the order of minutes. Any effects caused by forcing functions outside the frequency band of interest, such as tidal or internal wave effects, will not be considered. Thus it is necessary to eliminate the low frequency components in the raw data records. This was accomplished by using a Fourier Filter.

The first step is to generate a Fourier series of the record. The fast Fourier Transform algorithm is used to conserve computer time:

$$F(t) = \frac{A_0}{2} + \sum_{n=1}^{\infty} (A_n \cos n\omega t + B_n \sin n\omega t)$$

where F = parameter

t = time

$n\omega$ = nth harmonic of fundamental radial frequency ω

Next, a time series is generated using only the low frequency components that are to be eliminated. This time series, composed only of the low frequency components, is then subtracted from the original time series for each value, and the remainder is the filtered value of the parameter at each given time. In this experiment, the first fifteen low frequency components were used to generate the filtered time record, corresponding

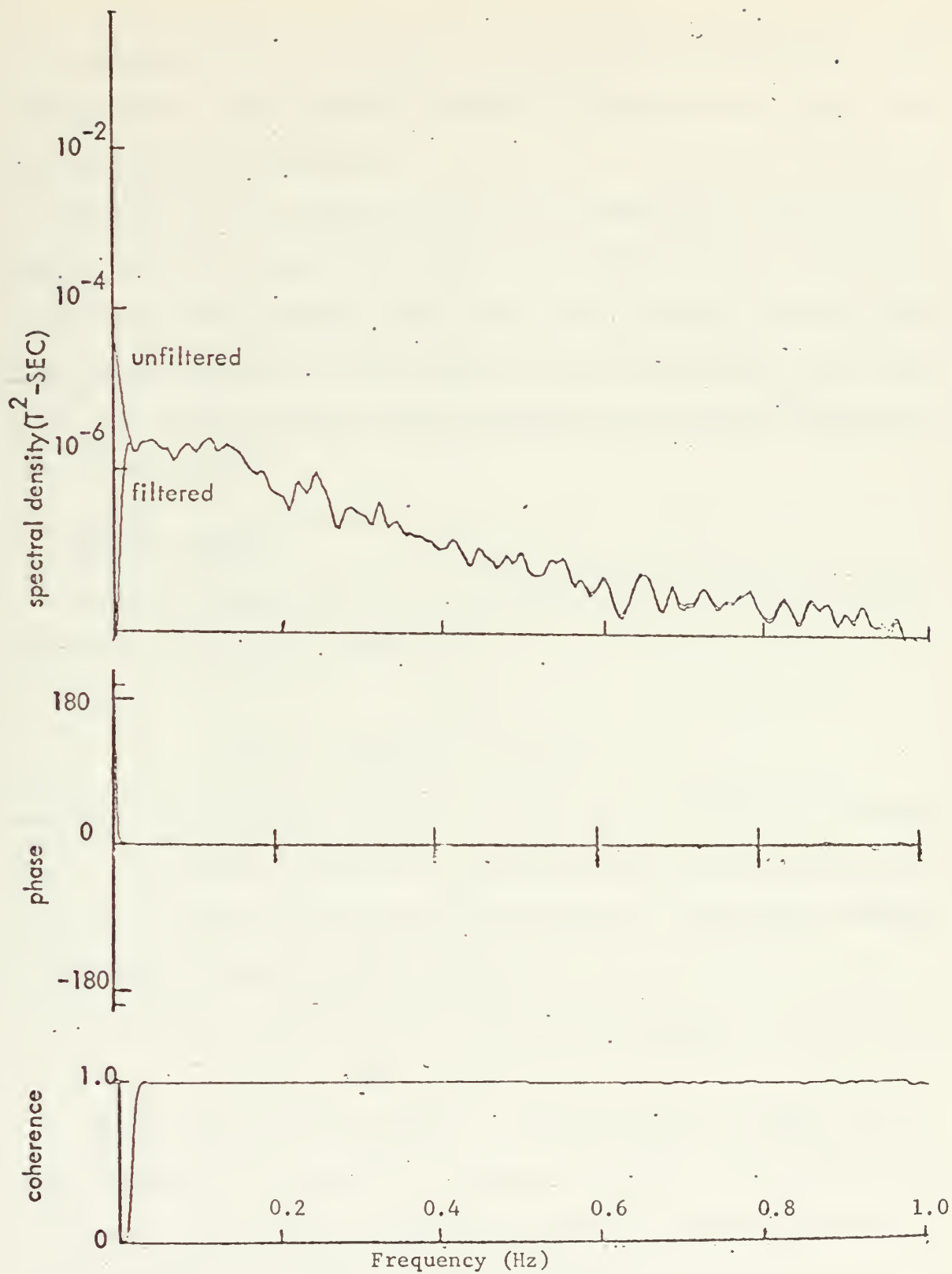


Figure 5. Filtered and Unfiltered Temperature 2 Spectra

to the components with a fifty-five second periodicity and greater. Although certain records needed filtering while others did not, all records were filtered for consistency.

The effect of the Fourier Filter on the temperature 2 spectra can be seen in Figure 5. Notice the removal of the energy from 0 to .018 Hz in the energy density spectrum. After this point, the energy spectra coincide for the remainder of the spectrum. Also of importance is that the phase and coherence spectra remain unaltered in the region of interest, greater than .018 Hz.

B. SPECTRAL ANALYSIS

The energy-density spectrum is calculated from the auto-covariance function of the recorded time series:

$$\phi_{11}(\tau) = \lim_{T \rightarrow \infty} \frac{1}{T} \int_t^{t+T} x_1(t) x_1(t + \tau) dt$$

where the auto-covariance function is expressed as a function of the lag time, τ . If the auto-covariance is normalized by division by the variance, it is called the auto-correlation function. The Fourier transform is the power or energy-density spectrum.

$$\hat{\phi}_{11}'(f) = \lim_{T \rightarrow \infty} \frac{1}{T} \int_{-T/2}^{T/2} \phi_{11}(\tau) e^{-i2\pi f\tau} d\tau$$

A Parzen lag window was applied to the functions to account for the finite length of the records in computing the spectra. Since the Parzen window has no negative side lobes, this eliminates any numerical instability problems that could arise in the analysis.

Let $P(\tau)$ denote the Parzen Window Function, then the modified energy density spectrum can be written:

$$\bar{\phi}_{11}(f) = \int_{-\infty}^{\infty} P(\tau) \phi_{11}(\tau) e^{-i2\pi f\tau} d\tau$$

The energy-density spectrum is the statistical estimate of the energy-density distributed over the frequency bands of the spectrum. The total potential energy-density of the sea surface height is proportional to the total area under the wave height spectrum. Similarly, the area under the velocity spectrum is proportional to the kinetic energy-density. The area under each curve is equal to twice the variance of the random variable.

The cross-spectral density is defined as the Fourier transform of the cross-covariance function. The cross-covariance function is similar to the auto-covariance function except that a second time series record is lagged against the first instead of a single record lagged against itself. The cross-covariance function indicates the dependence the values of one record have on that of another for various lag times. The cross-covariance function is:

$$\phi_{12}(\tau) = \lim_{T \rightarrow \infty} \frac{1}{T} \int_{-T/2}^{T/2} x_1(t) x_2(t + \tau) dt$$

The modified cross spectral density is:

$$\bar{\phi}_{12}(f) = \int_{-\infty}^{\infty} P(\tau) \phi_{12}(\tau) e^{-i2\pi f\tau} d\tau$$

The cross-spectrum can be defined in terms of its real and imaginary parts:

$$\bar{\phi}_{12}(f) = C_{12}(f) - iQ_{12}(f)$$

where the real part of $\bar{\phi}_{12}(f)$ is known as the co-spectrum:

$$C_{12}(f) = 2 \int_0^{\infty} [\bar{\phi}_{12}(\tau) + \bar{\phi}_{12}(-\tau)] \cos(2\pi f\tau) d\tau$$

and the imaginary part of $\bar{\epsilon}_{12}(f)$ is the quadrature spectrum:

$$Q_{12}(f) = 2 \int_0^{\infty} [\bar{\epsilon}_{12}(\tau) + \bar{\epsilon}_{12}(-\tau)] \sin(2\pi f\tau) d\tau$$

The spectral phase angle represents the average angular difference by which the cross correlated components of $x_2(t)$ lead those of $x_1(t)$ in each spectral frequency band. The phase angle is defined by:

$$\epsilon_{12}(f) = \arctan \left[\frac{Q_{12}(f)}{C_{12}(f)} \right]$$

$\epsilon_{12}(f)$ ranges from -180° to $+180^\circ$.

The coherence function is defined by:

$$\gamma_{12}^2(f) = \frac{[\bar{\epsilon}_{12}(f)]^2}{\bar{\epsilon}_{11}(f)\bar{\epsilon}_{22}(f)}$$

with the provision that:

$$|\bar{\epsilon}_{12}(f)| \leq \bar{\epsilon}_{11}(f)\bar{\epsilon}_{22}(f)$$

which results in:

$$0 \leq \gamma_{12}^2(f) \leq 1$$

The coherency spectrum is a measure of the correlation between two time series as a function of frequency. Three possible causes of coherency values being less than unity are: the system is not linear, excess noise is present in the measurement, or the output time series is due to the input time series as well as other functions (Bendat and Piersol [1]).

C. SPATIAL CORRELATION

The data were measured as a time series record at specific points in space. The majority of theory in this area of study requires knowledge of spatial correlations. Hence, meaningful comparisons cannot be made without measures of spatial correlations. The operation described below

is designed to convert the time domain record to a spatial one. The temporal measurements are transformed to a Lagrangian frame knowing the velocity and acceleration at the point of parameter measurement.

It is assumed a priori that the correlation lengths are small compared to the spatial scales of motion. At 7.3 meters depth the orbital excursion of a 10 second wave having a rms wave height of 30 centimeters (mean conditions during experiment) is 80 centimeters. It is further assumed that the temperature field is isotropic to simplify the analysis. Measurements of velocity in the X and Z plane were taken simultaneously along with temperature. Although the velocity components were measured a small distance from the thermistor it is consistent to assume that the velocity components can be transferred to the thermistor location, r_o , due to the small separation distance involved. If one now considers the thermistor moving with the velocity, U, and acceleration components, it will travel a path in the X-Z plane. At each instant the velocity is measured, the distance traveled by the thermistor, r, is calculated by

$$r = r_o + \frac{\Delta U \Delta t^2}{2\Delta t} + U\Delta t \quad (C-1)$$

(Δt = time increment)

whereupon the next temperature is assigned to this distance "r." Thus an array is created where a temperature is assigned for a certain distance "r" in the X-Z plane. For each temperature measurement in time there is an associated distance giving $T(r,t)$. In order to facilitate calculation of the auto-correlation function, any holes in the array were filled by linearly averaging the temperature over the distance increment.

The question arises as to the validity of the concept in relation to the occurrence of a negative velocity which would necessitate a backward

movement of the thermistor, bringing about the possibility of two different temperatures being assigned to the same point in the X-Z plane. The probability of this happening is small, and the effect of its occurrence is negated by averaging the first temperature with the second one. If by chance a third temperature were assigned this point, it would be averaged with the previously averaged temperature; hence the last temperature would always have a weighting factor of 50 per cent.

A similar scheme using an Eulerian frame can be derived by expanding the temporal measurement at a point in a Taylor series:

$$T(r,t) = T(r_0,t) + \frac{r\Delta T(r_0,t)}{\Delta r} + \frac{r^2\Delta^2 T(r_0,t)}{2\Delta r^2} + \dots \quad (C-2)$$

where $\Delta r = r - r_0$ and Δr is small. Employing Taylor's hypothesis that over short distances and time $U = \frac{\Delta r}{\Delta t}$, Equation (C-2) can be rewritten:

$$T(r,t) = T(r_0,t) + \frac{r\Delta T(r_0,t)}{U\Delta t} + \frac{r^2\Delta^2 T(r_0,t)}{2U^2\Delta t^2} + \dots \quad (C-3)$$

The two schemes are equivalent, but computationally the Lagrangian form is more convenient and is employed here.

D. AUTO-CORRELATION FUNCTION

With the conversion of a time series record to a spatial record in the preceding section, the description of the parameter in the medium by the spatial auto-correlation function is now possible. The importance of the spatial distribution of the parameter is illustrated in the following example. A sharp temperature boundary occurring within an acoustical wavelength of the propagated sound may cause reflection. The linear dimensions of the temperature inhomogeneity may cause scatter, reflection, or focusing of sound waves. The physical features of a parameter may be characterized by the auto-correlation function.

The computation of the spatial auto-correlation function, $\phi(\rho, t)$, from the temperature record, $T(r, t)$ is defined:

$$\phi(\rho, t) = \frac{\frac{1}{L} \int_{-L/2}^{L/2} T(r, t) \cdot T(r+\rho, t) dr}{\phi(0, t)} \quad (D-1)$$

where ρ is the lag distance and L , the total length of the field. Figure 6 shows the spatial auto-correlation function for temperature 1 and 2. Figure 7 shows the time auto-correlation function for the same parameters. Note the rapid decay to zero by both functions and also the sinusoidal components; thus both cases reveal the presence of periodic components, namely wave induced particle motions.

The distribution of temperature 2 in time is shown to closely approximate a Gaussian distribution in Figure 8, Figure 9 (using the Fourier Filter). Thus a good description for the function over short time lags would be:

$$\phi(t) = e^{-\frac{t^2}{t_0^2}} \quad (D-2)$$

where t_0 is the correlation time. Assuming a similar spatial Gaussian distribution gives:

$$\phi(\rho) = e^{-\frac{\rho^2}{\rho_0^2}} \quad (D-3)$$

The mean "size" of the inhomogeneities might reasonably be described by the value of ρ at which the temperature $\phi(\rho)$ drops to $1/e$ denoted by ρ_0 in Equation D-3. These distances are known as correlation distances (Liebermann [4]). For temperature records 1 and 2, their values of ρ_0 were 26 and 27 cm respectively.

The consistent results for correlation distances show that the conversion from time to the spatial domain is reasonable. Hence, the

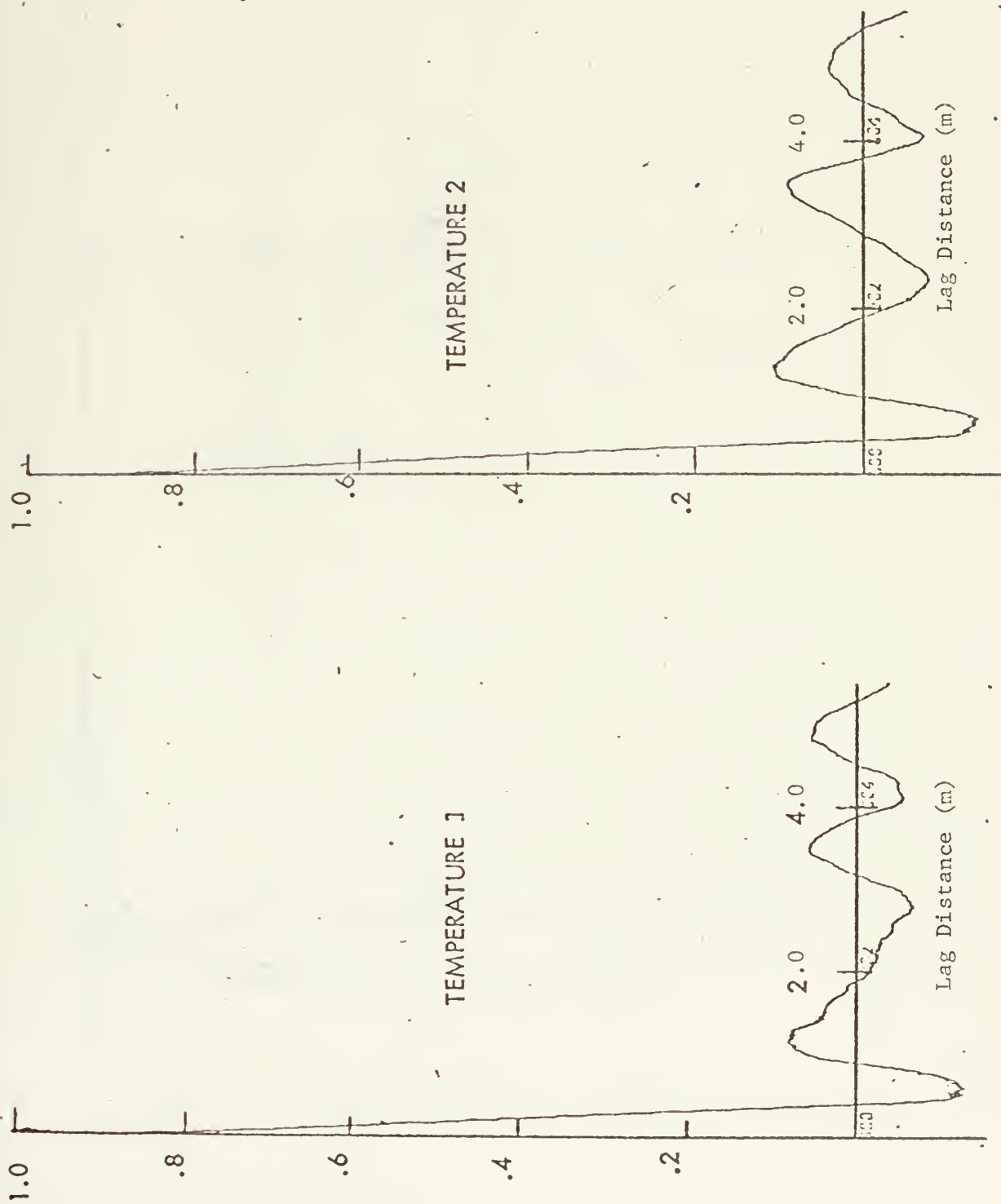


FIGURE 6 . SPATIAL TEMPERATURE AUTOCORRELATION FUNCTIONS



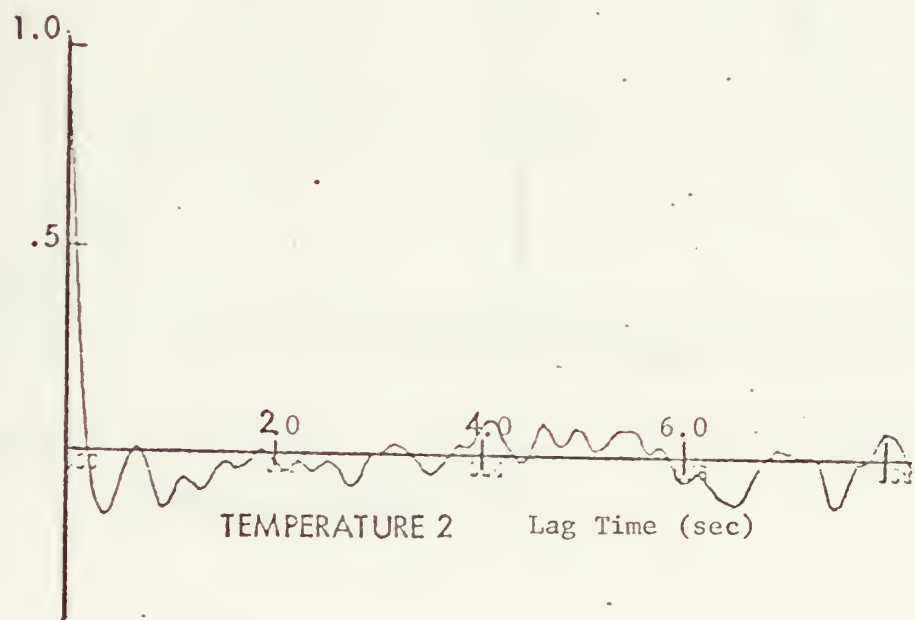
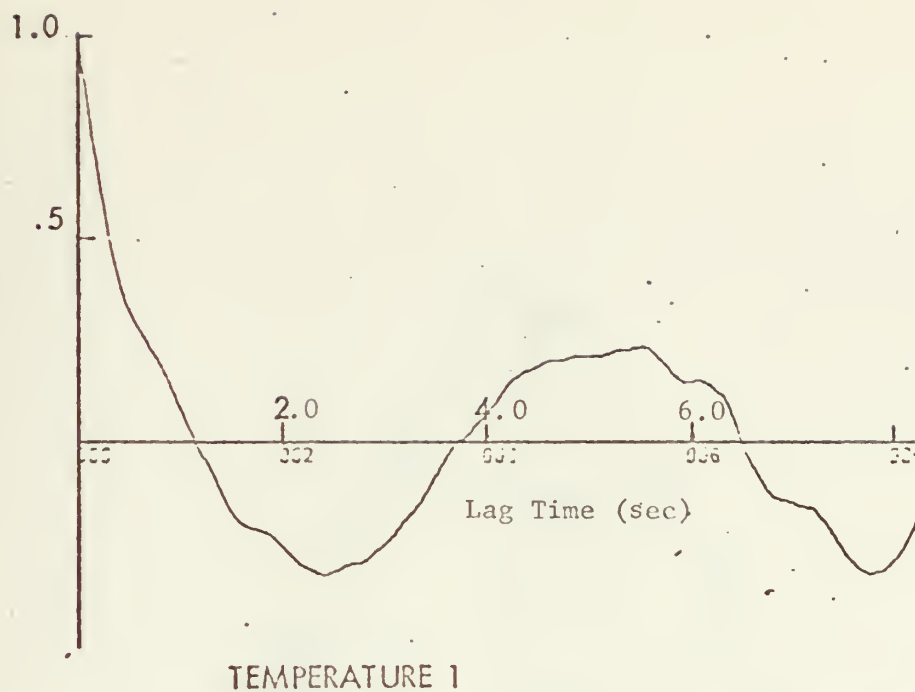


FIGURE 7 .TIME TEMPERATURE AUTOCORRELATION FUNCTIONS

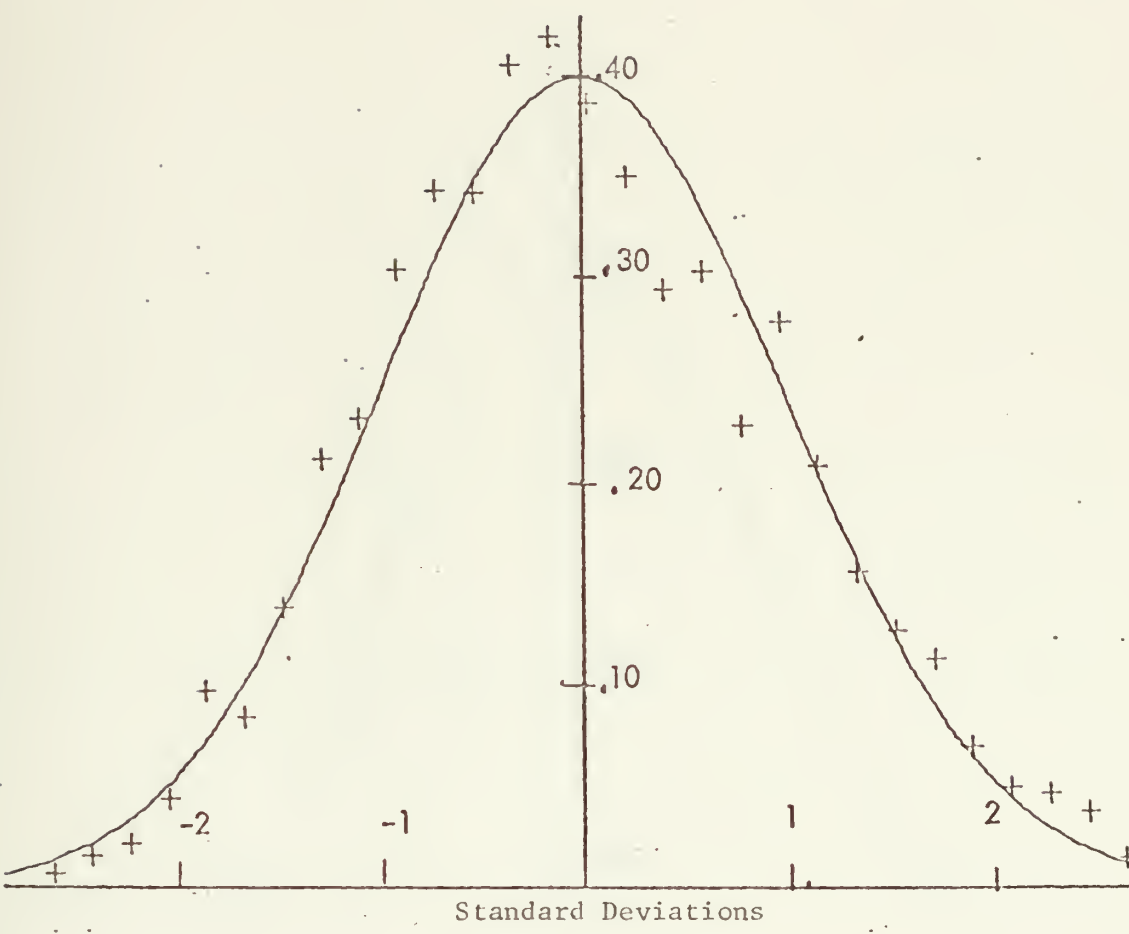


FIGURE 8. TEMPERATURE 2 PROBABILITY DENSITY FUNCTION WITHOUT FOURIER FILTER

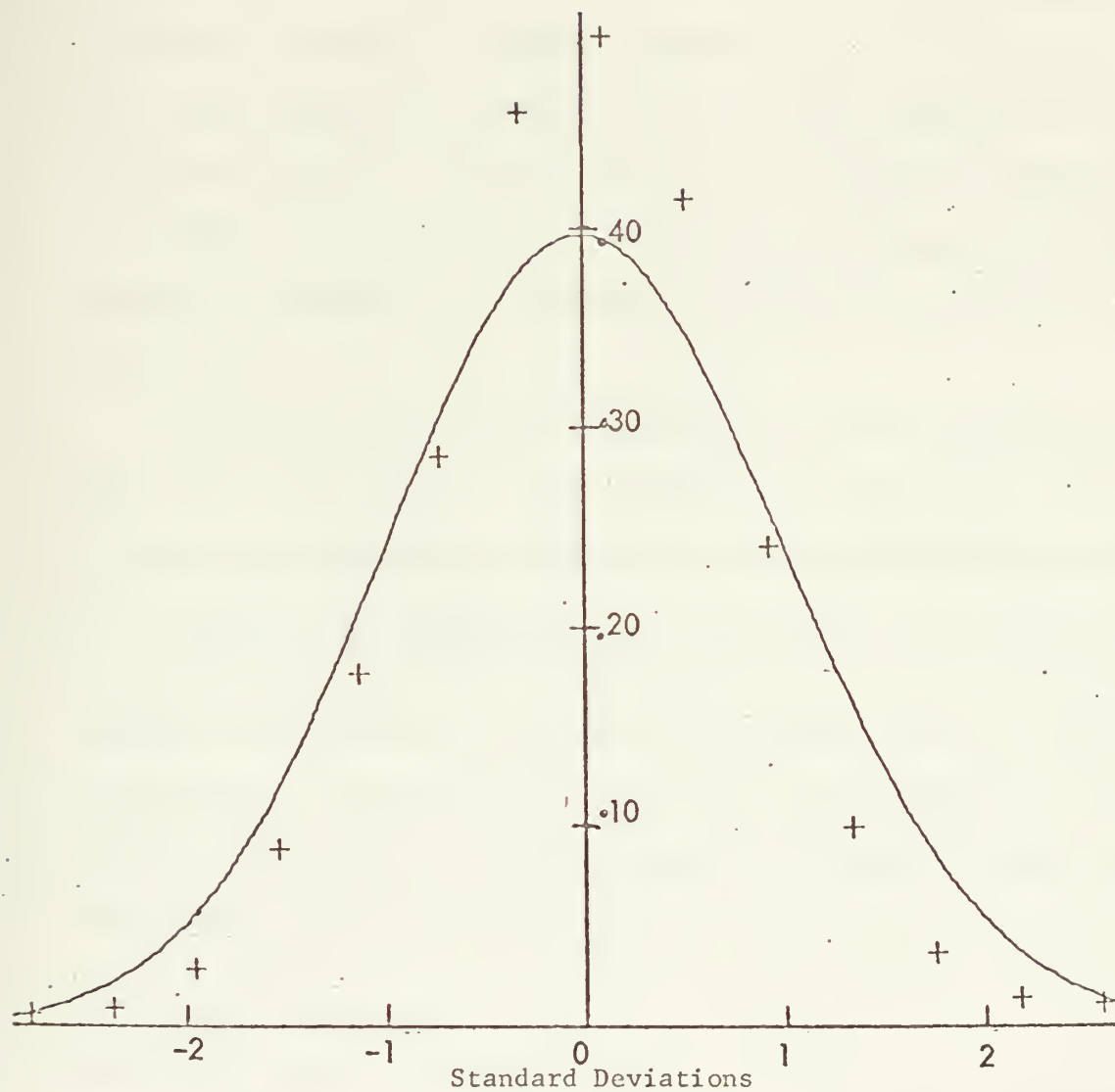


Figure 9. Temperature 2 Probability Density Function With Fourier Filter.

approximate mean size of the temperature inhomogeneities at a depth of 7.3 meters are characterized at about 26 centimeters. The difference in correlation times for temperature 1 and 2 as seen in Figure 7 (4.5 seconds versus 1.4 seconds) could be due to higher turbulence in the location of thermistor 2 which would result in smaller inhomogeneities. An alternative possibility would be a malfunction of the thermistor. Regardless, the conversion of a time series to a spatial domain has the effect of averaging out the localized turbulence by filling the spatial temperature array with smoothed values of temperature variations. Thus the spatial processing tends to average by minimizing the effect of localized turbulence.

A satisfactory distribution function for the near surface zone must take into account periodic motion induced by surface waves. Therefore, a more accurate description of the auto-correlation function would be:

$$\phi(\rho, t) = \left[e^{-\frac{\rho^2}{\rho_0^2}} \right] \left[\frac{A_0}{2} + \sum_{n=1}^{\infty} [A_n \cos n(kx - \sigma t) + B_n \sin n(kx - \sigma t)] \right]$$

However, this function is entirely too cumbersome. $R(\rho) = e^{-\frac{\rho^2}{\rho_0^2}}$ will be used because it describes the function very well through the correlation distance up to the first zero crossing and is capable of being integrated which is important in a later section.

E. WILSON'S EQUATION

Wilson's Equation [2] was originally developed to relate the speed of sound to the properties in ocean water that affect it, namely pressure, temperature, and salinity. An abbreviated form of Wilson's Equation is:

$$c = 1449 + 4.62T - 0.055T^2 + 0.0003T^3 + (1.39 - .012T)(s-35) + 0.017z$$

where c = speed of sound in meters per second

T = temperature in degrees Centigrade

s = salinity in parts per thousand

z = depth in meters

One of the initial aims of the experiment was to show that the variance of the speed of sound was equal to the sum of the variances of its constituents multiplied by their respective coefficients. This would establish the validity of Wilson's Equation in terms of variances as well as indicate the accuracy of the temperature, salinity, and depth data.

Wilson's Equation applied in this manner was not successful for the experiment. Let

$$\text{var } c = \langle (c - \bar{c})^2 \rangle$$

$$dT = \langle T - \bar{T} \rangle$$

$$ds = \langle s - \bar{s} \rangle$$

where the overbar implies averaging and $\langle \rangle$ indicates an ensemble average. After simplifying by retaining only first order terms of temperature and salinity and dropping the small depth term,

$$\text{var } c = \langle (5.04dT + 1.39 ds)^2 \rangle$$

$$\text{var } c = \langle (25.40dT^2 + 14.00 dT \cdot ds + 1.93ds^2) \rangle$$

and $dT \cdot ds = \text{covariance } (T \cdot s) = \text{cov } (T \cdot s)$.

In order to measure the variance of c using Wilson's Equation, both temperature and salinity must be measured at the same point at the same time. The time constant for the salinity sensor was .35 seconds, and for the thermistors .15 seconds. The average spatial distance between the instruments was 2.14 meters.

Correlation distance has been described in a previous section as representative of the mean size of the inhomogeneity. In order to ensure that temperature and salinity sensors provide accurate results,

they must be located within the same inhomogeneity along with the sound velocity meter. This is obtained only if all the instruments are placed within the smallest correlation distance of the parameters involved. Assuming that the mean size of a salinity inhomogeneity would be no smaller than that for temperature, then all instruments would have to have been placed within 26 centimeters in this experiment (as previously determined from temperature correlation distances) in order to provide an accurate evaluation of Wilson's Equation. For the experimental data taken, an application of Wilson's Equation in this case would be futile as Seymour [8] showed in his computer results.

As the distance between instruments increases in the random medium, one would expect that local mechanisms operating within one correlation distance to bear less and less resemblance to mechanisms operating at increased correlation distances; hence, the temperature and salinity would approach statistical independence with increasing distance, causing $\text{cov}(T's)$ to approach zero by definition. This was found to be the case in Run Five where the $\text{cov}(T's)$ integrated over the spectrum was found to be $-.8 \times 10^{-5} (\text{C}^\circ\text{-PPT})$. The variance of temperature was $1.6 \times 10^{-4} (\text{C}^\circ)^2$, the variance of salinity $0.22 \times 10^{-2} (\text{PPT})^2$, and the variance of sound velocity $1.1 \times 10^{-4} (\text{meters/second})^2$.

The importance of the waves to the variance of the parameters is indicated by band-pass filtering. Band-pass filtering was accomplished by high-pass filtering with the Fourier filter described before and calculating the variance by summing the spectral contributions only of frequencies up to 0.16 Hz. The band-pass filter was chosen because it included that part of the variance where organized wave-induced particle motion was dominant in its contribution to the variance, and the effects

of turbulence and instrument noise were insignificant. Table II shows the results of the band-pass filter.

TABLE II

VARIANCES OF SOUND VELOCITY, TEMPERATURE, AND SALINITY

Variance	Entire Spectrum	Band-pass Filter	% Variance in wave dom- inated region
var c	1.1×10^{-4}	1.0×10^{-4}	91%
var T	1.6×10^{-4}	0.6×10^{-4}	38%
var s	21.5×10^{-4}	19.1×10^{-4}	90%

On inspection, the high value of variance for salinity makes it questionable as one would expect a value of the same order of magnitude as the temperature, not 13 times as great. Further investigation indicates that the measured conductivity is compensated continuously for pressure and temperature changes with the result that the indicated salinity has a tendency to oscillate; thus the high value for the variance of salinity should be disregarded. This is significant in itself, and when combined with a lack of the covariance term, $\text{cov}(T \cdot s)$, it makes any proof of Wilson's Equation only conjecture. Hence, future investigations must use more appropriate salinity instrumentation in the near surface region of the ocean.

The frequency of the sound velocimeter was 4 MHz. In this frequency range, the bubbles present in the near surface zone have no effect on sound propagation due to the extremely small wavelength of the sound wave. Thus by measuring the variance of the sound velocimeter and comparing it by Wilson's Equation to the variances of the temperature, salinity and

their respective covariance, one gets a crosscheck on the refraction of sound in the medium due only to salinity and temperature.

F. AMPLITUDE MODULATION IN A RANDOM MEDIUM

In an ideal homogeneous undisturbed medium, a sound wave propagated at a fixed frequency and amplitude arrives in the far field undiminished except for spherical spreading and absorption losses. An adequate description of the process for a homogeneous medium is given by the general wave equation:

$$\nabla^2 P = 1/c^2 \frac{\partial^2 P}{\partial t^2} \quad (F-1)$$

where ∇^2 = LaPlacian operator

P = pressure

c = speed of propagation in medium.

The medium under study is the near surface ocean. Bubbles, temperature and salinity patches, and scatterers are all present in a random distribution. Compounding the problem is the fact that the inhomogeneities are in constant motion due to wave particle motion or convective forces. As the sound wave moves through a medium, the inhomogeneities cause a variation in the speed of sound which results in refraction. If the inhomogeneities were motionless, reflection and refraction of a propagating sound beam would cause the amplitude of the sound beam to be constant at a given receiver. If the inhomogeneities have freedom to move in and out of the path of the sound beam, then the amplitude of the sound beam at the receiver will fluctuate. Hence, the wave equation must be modified to include spatial and temporal changes in the speed of sound. The change in the index of refraction with time and space is defined:

$$\mu(\vec{r}, t) = \frac{c(\vec{r}, t)}{c_0} = \frac{c_0 + dc(\vec{r}, t)}{c_0} = 1 + \frac{dc(\vec{r}, t)}{c_0} = 1 + \alpha \quad (F-2)$$

where: $\alpha = \frac{dc(\vec{r}, t)}{c_0}$

μ = Index of refraction

c_0 = Average speed of sound

$c = c_0 + dc$ = Local speed of sound

α = RMS refractive index variation from unity

t = Time

\vec{r} = Position vector

Previous measurements of α for temperature inhomogeneities have yielded values such as 1.18×10^{-4} (Stone and Mintzer in Laboratory [10]) and 7.0×10^{-5} (Liebermann [6] in Ocean Experiments at depths of 50 meters). In Run Five of this experiment, the calculated α for temperature inhomogeneities at a depth of 7.3 meters was 3.0×10^{-5} . This was calculated by taking the first derivative of Wilson's Equation with respect to temperature and substituting the rms value of the temperature variance into only temperature terms up to the third order; the average speed of sound was calculated using Wilson's Equation with time averaged values for temperature, salinity, and pressure. In comparing Liebermann's results to Run Five, the implication is that the temperature inhomogeneities are smaller near the surface. This seems reasonable as water particle motion caused by wave action decays exponentially with depth; hence better mixing would be expected nearer the surface reducing the size of the temperature inhomogeneities.

In their laboratory studies of amplitude modulation in a random medium, Mintzer and Stone, [6], defined the coefficient of variation, cv:

$$(cv)^2 = \frac{(\langle P^2 \rangle - \langle P \rangle^2)}{\langle P \rangle^2} \quad (F-3)$$

where, cv = The coefficient of variation

P = The amplitude of the received signal

The coefficient of variation as defined by Mintzer and Stone is related to the fractional modulation measured in Run Five by the following equation:

$$(.0253)(cv)^2 = \text{var Modulation}$$

The development of this relationship is found in Appendix I of Smith [9].

The majority of theory dealing with propagation in a moderately inhomogeneous medium employs the single scattering approximation to the wave equation. Mintzer and Stone [6] have shown that:

$$(cv)^2 = \alpha^2 K_o^2 b \int_0^{\infty} \phi(\rho) d\rho \quad (F-4)$$

where:

K_o = Wave number

b = range from source to receiver

$\phi(\rho)$ = the correlation function taken along the path from source to receiver.

α = root mean square index of refraction variation from unity.

Previously, it was determined that the temperature auto-correlation was described by $\phi(\rho) = e^{-\frac{\rho^2}{\rho_o^2}}$. Other parameters affecting the index of refraction showed similar Gaussian distributions; therefore, substituting the expression for $\phi(\rho)$ (representing a combined temperature, salinity and bubble inhomogeneity auto correlation function) into equation (F-4) and integrating, one gets the following result:

$$(cv)^2 = \frac{1}{2} \sqrt{\pi} K_o^2 \alpha^2 \rho_o^2 \quad (F-5)$$

In Run Five the sound modulation was obtained for a sound wave of frequency 60 kHz. This frequency has a wavelength of 2.5 centimeters

which happens to correspond to a peak in the resonant bubble regime of the near surface zone at a depth of 7.3 meters in this experiment, as determined from Rautmann [7]. By using two hydrophones to determine phase change over a 78 cm path, Rautmann converted the phase change to a change in the speed of sound. At 7.3 meters depth during the same 18 hour time period, an interpolated value for 60 kHz from Rautmann's tables indicates $c(\text{measured}) - c(\text{theoretical}) = -1 \text{ m/sec}$. $C(\text{measured})$ is the speed of sound based on phase measurements while $c(\text{theoretical})$ is taken from Wilson's Equation using average temperature, salinity, and depth. Thus the variance of the speed of sound at 60 kHz was determined to be $1 (\text{m/sec})^2$ due to temperature, salinity, and bubble inhomogeneities.

Converting this to an α value gives the relatively high value of $.67 \times 10^{-3}$. This value is based on bubbles, temperature, and salinity, not just temperature alone which gave a value of $.25 \times 10^{-5}$. Since the salinity values were highly suspect and along with the lack of a $\text{cov}\langle T \cdot s \rangle$ term, one cannot accurately determine the exact effect of bubbles on α . However if one makes the modest assumption that the salinity contribution to $dT \cdot ds$ will be equal to the temperature contribution or less, then the temperature and salinity contribute less than one percent of the value of α . This shows the enormous importance of bubbles in the near surface region upon the refraction of sound at 60 kHz.

Further proof of the importance of bubbles can be seen in the spectral analysis of wave height versus temperature, salinity, and sound modulation (see Figures 10, 11, and 12). In the coherence and phase spectra of wave height versus temperature and salinity, small consistent values of coherence and phase are found in the wave dominant portion of the spectrum (.05 to .22 Hz). However, for wave height versus sound modulation,

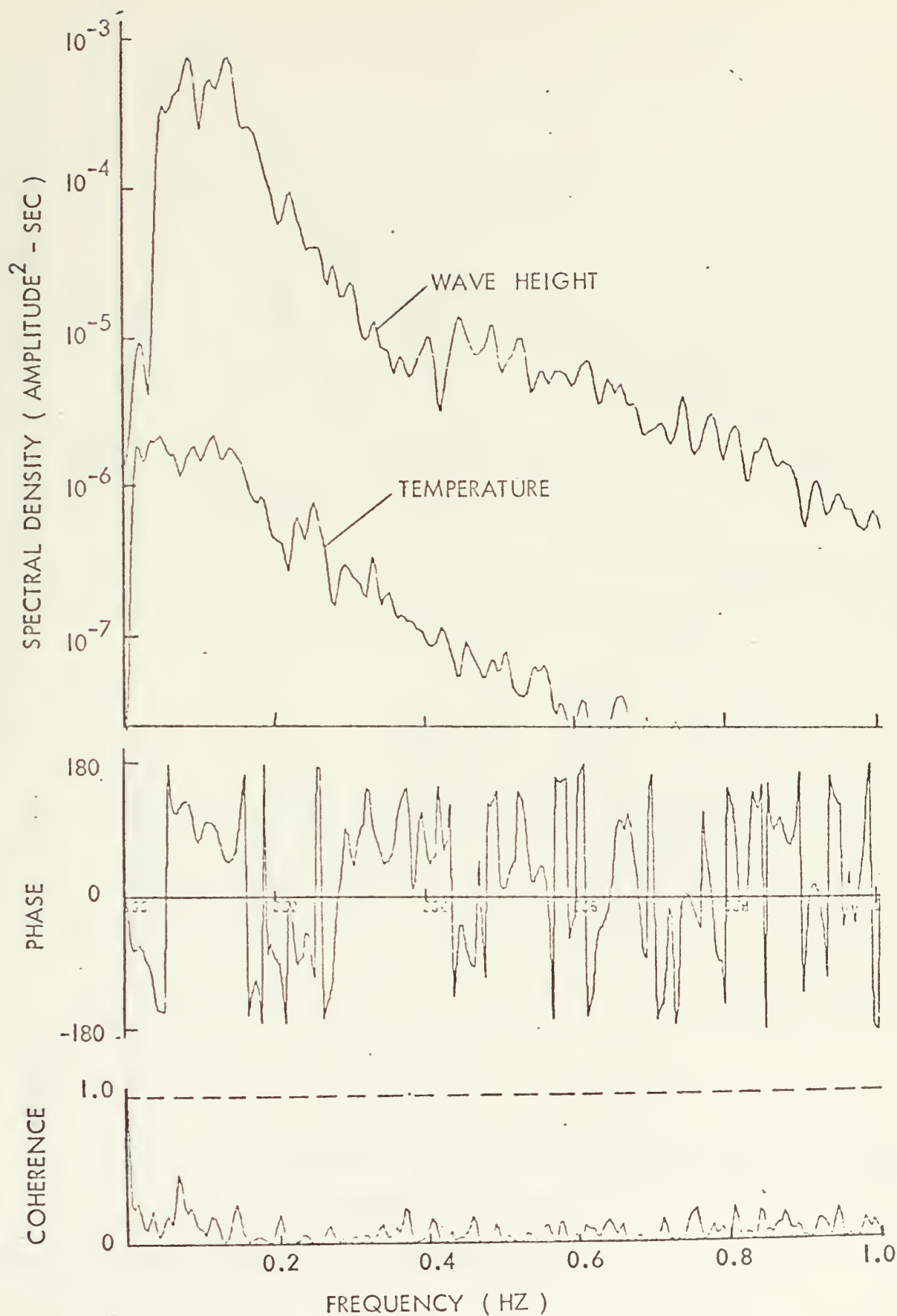


FIGURE 10 . WAVE HEIGHT AND TEMPERATURE - 2 SPECTRA

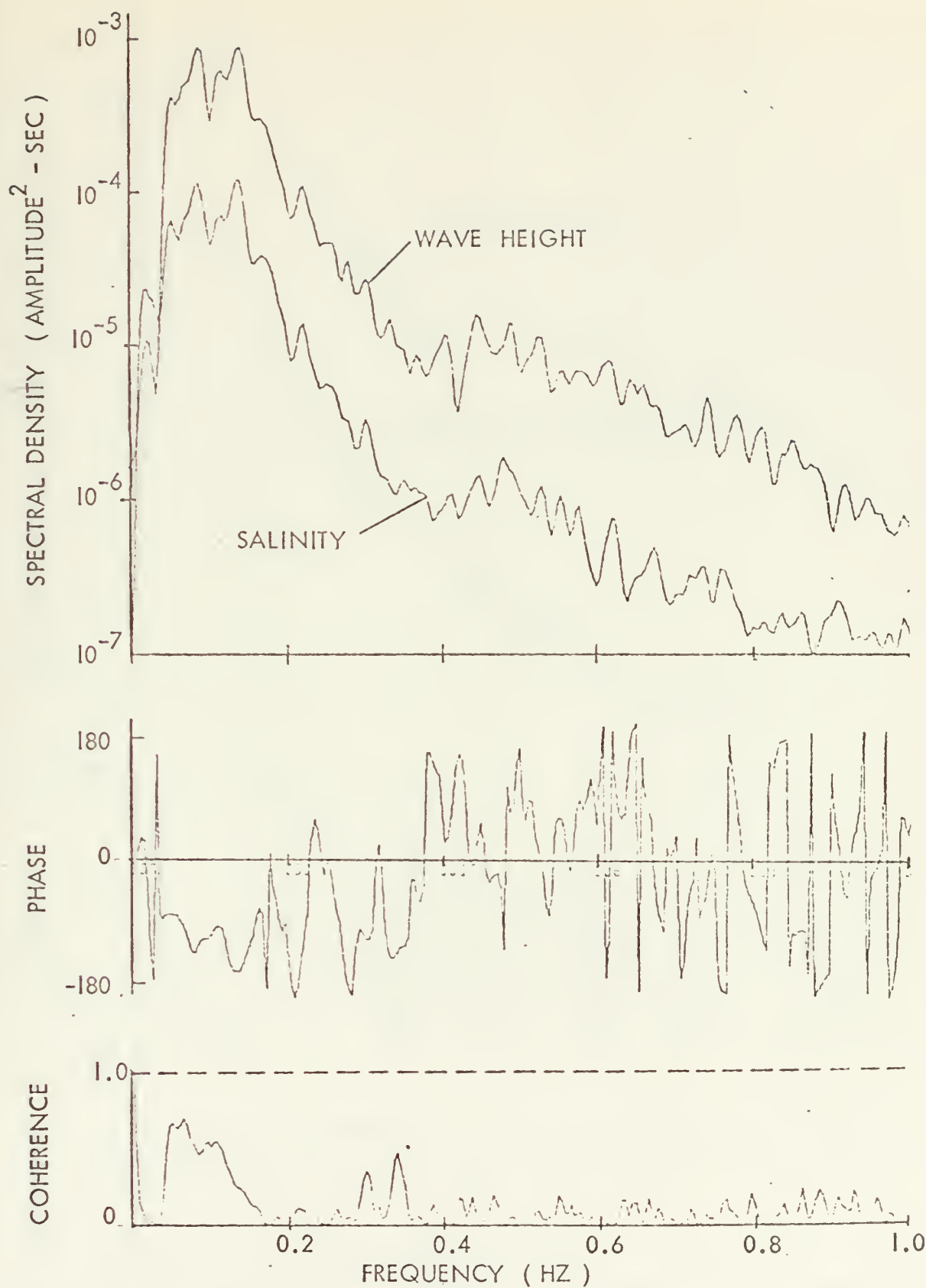


FIGURE 11. WAVE HEIGHT AND SALINITY SPECTRA

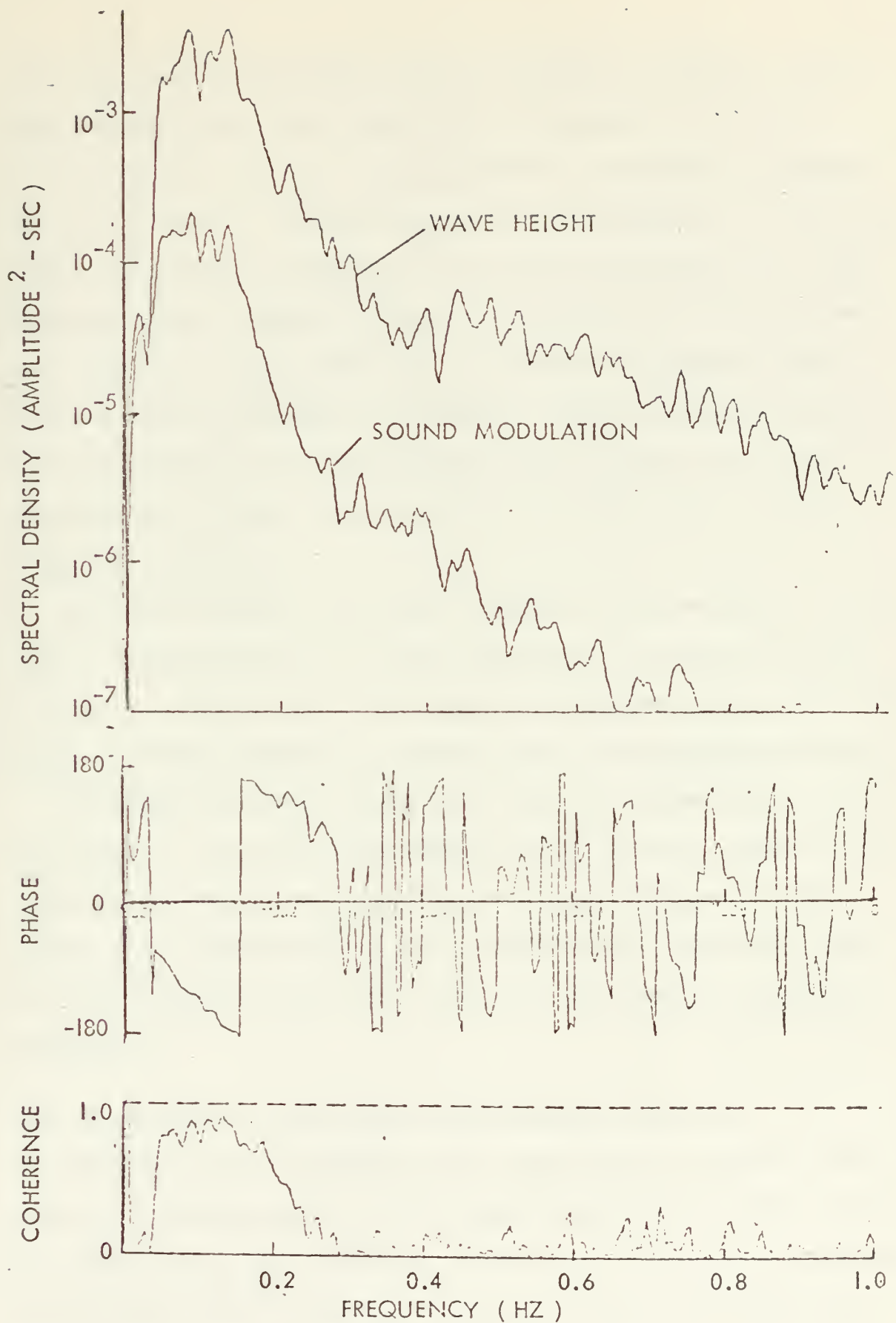


FIGURE 12 . WAVE HEIGHT AND SOUND MODULATION SPECTRA

the coherence value approaches unity and the phase is constant in the wave dominant region. This implies that wave height is linearly related to sound modulation. Since the effect of the change in pressure due to wave height is insignificant on the sound modulation at this depth then the fluctuation in modulation must be due to the variations in the inhomogeneities. With the coherence of wave height and temperature and wave height and salinity being low, the process of elimination leaves only one type of inhomogeneity -- bubbles. This supports the contention for this experiment that the dominating cause of change in the speed of sound was due to bubbles as evidenced by very high coherence of wave height and modulation.

This high coherence can be due to two wave related mechanisms: 1) the bubbles (inhomogeneities) are moved in and out of the sound path by the wave induced motion and, 2) the bubbles are "squeezed" by the wave induced pressure changes resulting in a change in their resonance characteristics.

In applying the data from Run Five to Mintzer's equation, " ρ_0 ," the mean radius of the scattering inhomogeneity, is found to be equal to 8.8 centimeters. This is not to say that an inhomogeneity exists with a radius of 8.8 centimeters, but the effect of bubbles, temperature, and salinity provides an "effective" radius of 8.8 centimeters for the inhomogeneity.

G. THE EFFECTS OF SURFACE WAVES ON THE MEASURED PARAMETERS

There are three contributors to the energy density spectrum of horizontal or vertical particle motion: wave induced particle motion, mean convective motion, and turbulence. Mean convective motion was essentially zero for the particle velocity in the vertical plane. This leaves wave



induced particle motion and turbulence as the two dominant sources in supplying energy to the power spectrum of vertical particle motion.

Turbulence is random three-dimensional motion which can dissipate mechanical energy to internal energy through a cascade of eddies of diminishing size. The process of turbulent cascade, resulting in dissipation, includes nonlinearity and three dimensionality as well as rotationality. In contrast to this is wave induced particle motion which, while being random and three dimensional, is approximately irrotational and nondissipative (Lumley and Panofsky [5]). Figure 13 clearly establishes the irrotationality of the wave induced velocities by showing an almost constant phase difference of 90° between u and w components in the region of significant energy density. The 90° phase difference is predicted by solving the linear first order wave equation in terms of velocity potential. A qualifying condition for a velocity potential is the existence of irrotationality in the fluid.

The horizontal component of water particle velocity, u, will not be considered in terms of absolute or quantitative values as the velocity meter measured only one component of the horizontal velocity during Run Five.

The measured energy-density spectrum of the vertical water particle velocity has been plotted in Figure 14. Figure 14 also shows the calculated values of the vertical velocity energy-density spectrum predicted using linear wave theory (Bordy [2]):

$$|w(f)|^2 = \left[\frac{f}{2\pi} \frac{\sinh k(h+z)}{\sinh kh} \right]^2 |\eta(f)|^2$$

The term in brackets is the first order vertical velocity amplitude - response function squared. η is a measure of wave height as a function

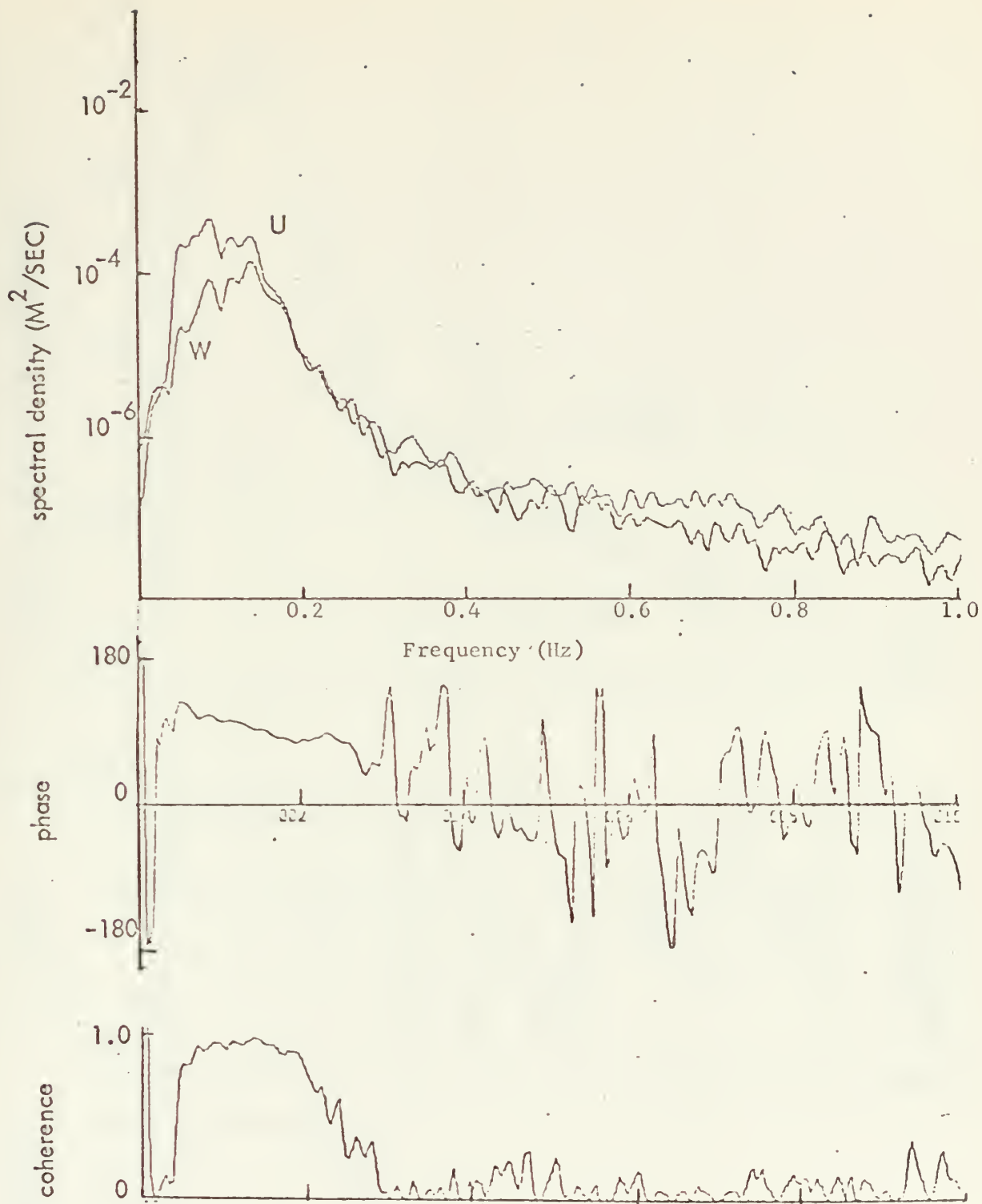
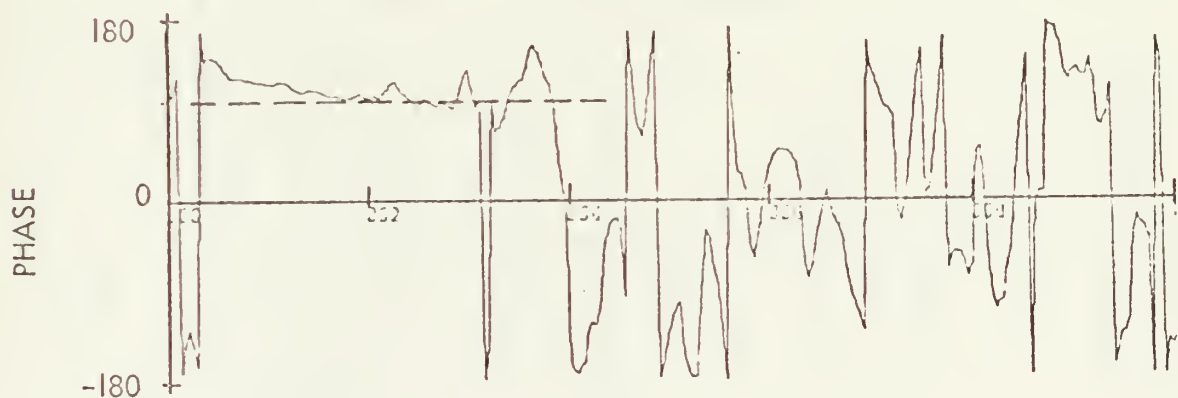
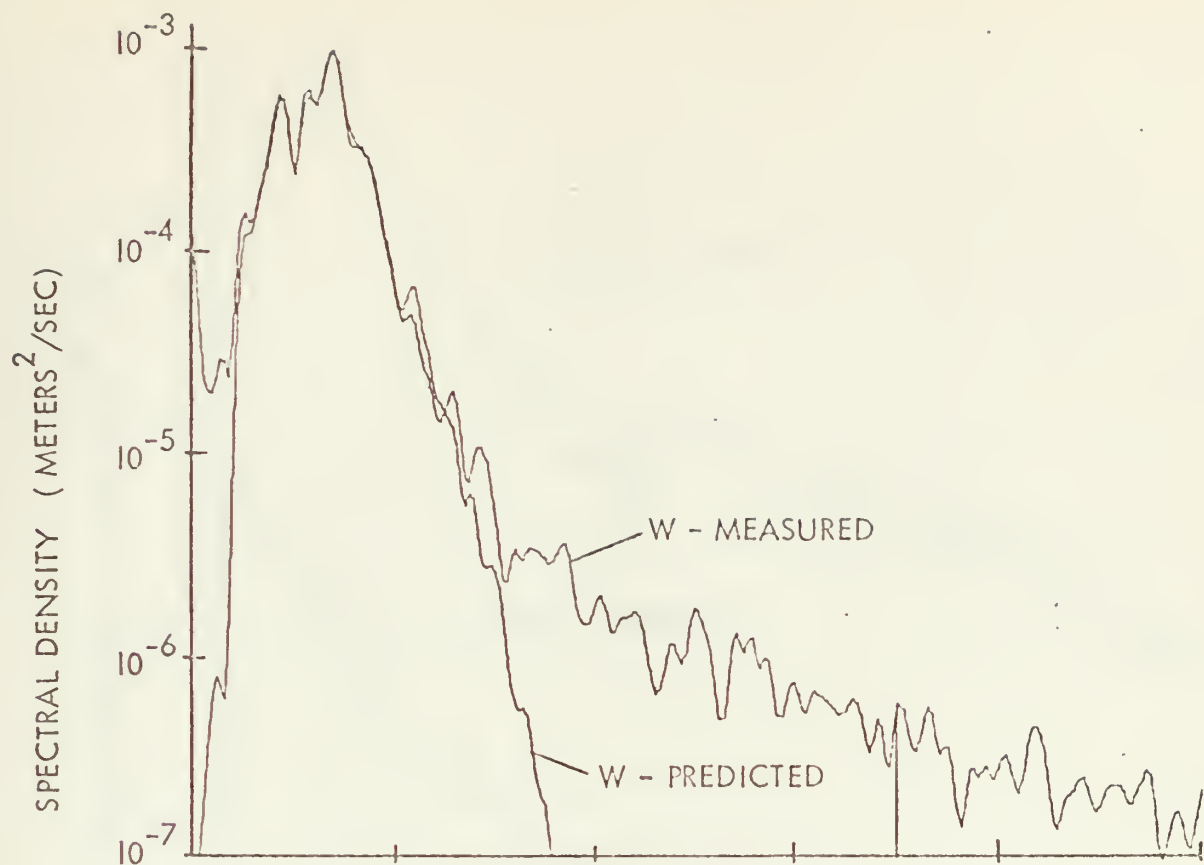


Figure 13. U and W Velocity Component Spectra.



* Phase and Coherence Spectra Represent Wave Height versus W-measured.

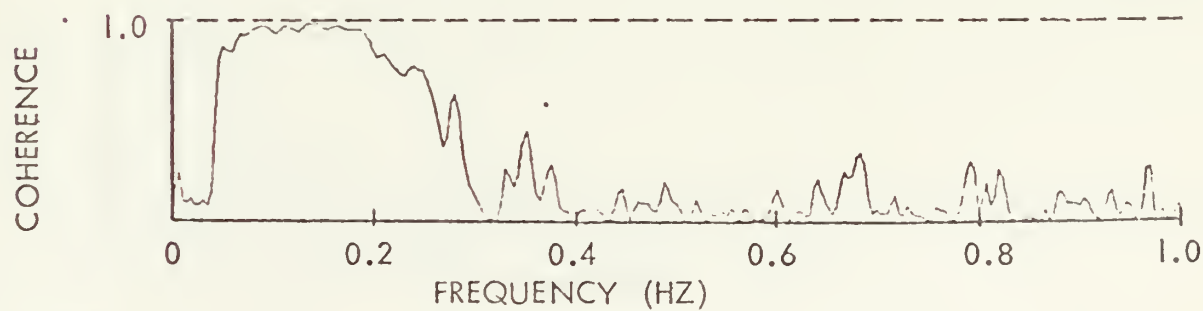


FIGURE 14. MEASURED AND THEORETICAL VERTICAL VELOCITIES

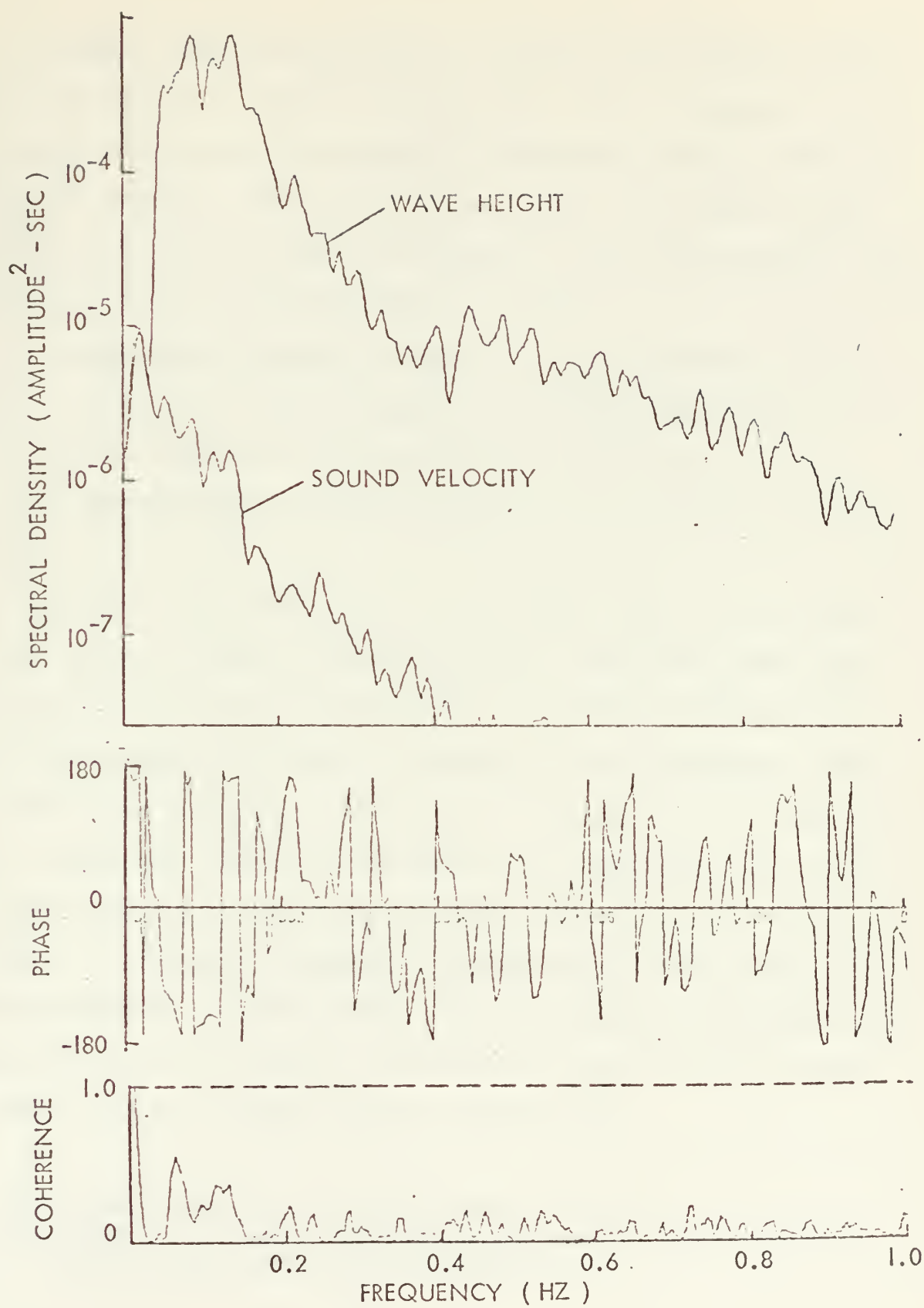


FIGURE 15 . WAVE HEIGHT AND SOUND VELOCITY SPECTRA

of frequency. The measured velocity was equal to the theoretical value for the region of significant energy-density. Close examination of the spectra indicates that the measured and theoretical vertical velocities begin to diverge at a frequency of about 0.2 Hz. This marks the beginning of the transition regime to turbulence. At 0.3 Hz turbulence is the dominant process in the energy density spectrum.

Spectra of other parameters compared to waves are shown in Figures 10, 11, 12, and 15. The contribution to the energy-density spectra of each by wave induced particle motion in the frequency range .05 Hz to .22 Hz approaches 95% of the total energy with the exception of temperature.

The phase and coherence spectra of the wave height versus modulation, shows the coherence approaching unity. This strong linear relationship of waves and sound modulation was attributed to bubbles in an earlier section. The values of coherence are less for salinity, sound velocity, and temperature, with the least coherence for wave height versus temperature. This could indicate that the temperature scalar field is more affected by turbulence and thermal diffusivity*, or it could indicate an instrumental inadequacy. Regardless, it is noted that the temperature has a significantly less linear relationship with wave height than the other parameters and accordingly only about 40% of its energy comes in the wave dominant portion of the spectrum.

* The thermal diffusivity is approximately 10 times greater than salt diffusivity in the ocean. Thus temperature gradients are expected to be erased much quicker than salinity gradients.

VI. CONCLUSIONS

- A. The Fourier high pass filter proved to be an effective method of eliminating low frequency components from the signal record without altering phase, coherence, or energy relationships in the region of interest.
- B. The spatial correlation distances for temperature determined for measurements at a point were established to be about 25 centimeters.
- C. Future experiments attempting to verify Wilson's equation by summing the variances of its constituents (T,s,P) should require the instruments to be placed within a correlation distance; this insures that the local mechanisms affecting temperature and salinity inhomogeneities are identical and will give a valid covariance term. Further, better salinity instrumentation is required for the time scales considered in the near surface region.
- D. Sound modulation of a 60 kHz sound beam traversing a 2 meter path length underwent a mean attenuation of about 5%. The correlation distance of an effective inhomogeneity due to the combined temperature, salinity, and bubble effects was found to be 8.8 centimeters by applying Mintzer and Stone's Equation.
- E. The change in the index of the speed of sound at 60 kHz (a resonant bubble region) was found to be 99% induced by bubbles.
- F. The energy density spectra of all parameters were dominated by wave induced motion at 7.3 meters depth.

G. High coherence is found between wave induced water particle motion and sound modulation and decreasing coherence between water particle motion and salinity, sound velocity, and temperature.

H. First order wave theory accurately predicts orbital water particle velocities.

I. Wave induced water particle velocities are irrotational.

BIBLIOGRAPHY

1. Bendat, K. R., and A.G. Pierson, Measurement and Analysis of Random Data, Wiley, 1966.
2. Bordy, M.W., Spectral Measurement of Water Particle Velocities Under Waves, MS Thesis, United States Naval Postgraduate School, Monterey, 1972.
3. Duchock, C.J., The Measurement and Correlation of Sound Velocity and Temperature Fluctuations Near the Sea Surface, MS Thesis, United States Naval Postgraduate School, Monterey, 1972.
4. Liebermann, L., "The Effect of Temperature Inhomogeneities in the Ocean on the Propagation of Sound," The Journal of the Acoustical Society of America, v. 23, p. 563 - 570, September 1951.
5. Lumley, J.L., and Panofsky, H. A., The Structure of Atmospheric Turbulence, Wiley, 1964.
6. Mintzer, D. and Stone, R.G., "Transition Regime for Acoustic Fluctuations in a Randomly Inhomogeneous Medium," Journal of the Acoustical Society of America, v. 38, p. 843 - 846, November 1965.
7. Rautmann, J., Sound Dispersion and Phase Fluctuations in the Upper Ocean, MS Thesis, United States Naval Postgraduate School, Monterey, 1971.
8. Seymour, H. A., Statistical Relations Between Salinity, Temperature, and Speed of Sound in the Upper Ocean, MS Thesis, United States Naval Postgraduate School, Monterey, 1971.
9. Smith, W. J., Jr., Amplitude Modulation of an Acoustic Wave Propagating Near the Ocean Surface, MS Thesis, United States Naval Postgraduate School, Monterey, 1971.
10. Wilson, W. D., "Speed of Sound in Sea Water as a Function of Temperature, Pressure, and Salinity," The Journal of the Acoustical Society of America, v. 32, p. 641 - 644, June 1960.

INITIAL DISTRIBUTION LIST

	No. Copies
1. Defense Documentation Center Cameron Station Alexandria, Virginia 22314	2
2. Library, Code 0212 Naval Postgraduate School Monterey, California 93940	2
3. Oceanographer of the Navy The Madison Building 732 N. Washington Street Alexandria, Virginia 22217	1
4. Department of Oceanography Naval Postgraduate School Monterey, California 93940	3
5. Commander, Navy Ship Systems Command Code 901 Department of the Navy Washington, D.C. 20305	1
6. Dr. Ned A. Ostenso Deputy Director (acting) Code 480 D Ocean Science and Technology Division Office of Naval Research Arlington, Virginia 22217	1
7. Dr. Albert D. Kirwan, Jr. Program Director/ Physical Oceanography Code 481 Ocean Science and Technology Division Office of Naval Research Arlington, Virginia 22217	1
8. LCDR Jon W. Carlmark (USN) Project Office Code 485 Ocean Science and Technology Division Office of Naval Research Arlington, Virginia 22217	1
9. Professor H. Medwin, Code 61 Department of Physics Naval Postgraduate School Monterey, California 93940	1

	No. Copies
10. Dr. Noel E. Boston, Code 58 Department of Oceanography Naval Postgraduate School Monterey, California 93940	1
11. LT. Mark C. Haley, USN USS DRUM SSN - 677 FPO San Francisco, California 96601	3
12. CDR. John D. Peters, USN Commanding Officer USS JOHN ADAMS SSBN 620 BLUE FPO San Francisco, California 96601	1
13. Professor David Mintzer Technological Institute Northwestern University Evanston, Illinois	1
14. Dr. E. B. Thornton, Code 58 (Thesis Advisor) Department of Oceanography Naval Postgraduate School Monterey, California 93940	5
15. Mr. Thomas F. Haley 18 Bennett Place Westfield, New Jersey 07090	1
16. LCDR. C. K. Roberts USN Department of Oceanography, Code 58 Naval Postgraduate School Monterey, California 93940	1
17. Pete Mandics WPL R45x8 NOAA/ERL Boulder, Colorado 80303	1
18. Mr. L. A. Vega University of California, San Diego Dept. of AMES P.O. Box 109 La Jolla, California 92037	1
19. Dr. Thorleif Strand Department of Port and Ocean Engineering Technical University of Norway Trondheim, Norway	1

UNCLASSIFIED

Security Classification

DOCUMENT CONTROL DATA - R & D

Security classification of title, body of abstract and indexing annotation must be entered when the overall report is classified

ORIGINATING ACTIVITY (Corporate author)

Naval Postgraduate School
Monterey, California 93940

2a. REPORT SECURITY CLASSIFICATION

Unclassified

2b. GROUP

REPORT TITLE

Small Scale Interactions in the Near Surface Ocean

DESCRIPTIVE NOTES (Type of report and, inclusive dates)

Master's Thesis; December 1972

AUTHOR(S) (First name, middle initial, last name)

Mark Christopher Haley

REPORT DATE

December, 1972

7a. TOTAL NO. OF PAGES

57

7b. NO. OF REFS

10

a. CONTRACT OR GRANT NO.

b. PROJECT NO.

9a. ORIGINATOR'S REPORT NUMBER(S)

9b. OTHER REPORT NO(S) (Any other numbers that may be assigned this report)

10. DISTRIBUTION STATEMENT

Approved for public release; distribution unlimited.

11. SUPPLEMENTARY NOTES

12. SPONSORING MILITARY ACTIVITY

Naval Postgraduate School
Monterey, California 93940

13. ABSTRACT

Experiments were conducted at the NURDC oceanographic tower off San Diego, California to describe the small scale physical properties in the upper ocean and to determine their temporal and spatial interrelationships. The measured parameters included water particle velocities, temperatures, salinity, sound speed, sound speed (phase) modulation, sound amplitude modulation and surface waves. Simultaneous time series measurements are analyzed for a twenty minute record taken at a depth of 7.3 m. The spatial correlation distance for temperature was found to be about 25 cm. Sound modulation of a 60 kHz sound beam underwent a mean attenuation of about 5%. The correlation distance of an effective inhomogeneity due to the combined temperature, salinity, and bubble effects was found to be 8.8 cm. The change in the index of refraction of the speed of sound at 60 kHz (a bubble resonant region) was found to be 99% induced by bubbles. The energy density spectra were dominated by wave induced motion. First order wave theory accurately predicts orbital water particle motion and its irrotationality. High coherence is found between wave-induced water particle motion and sound modulation and decreasing coherence between water particle motion and salinity, sound velocity, and temperature.

KEY WORDS

Fourier filter

141631

Thesis
H143
c.1

Haley
Small scale inter-
actions in the near
surface ocean.

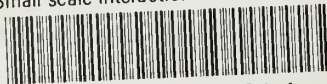
141631

Thesis
H143
c.1

Haley
Small scale inter-
actions in the near
surface ocean.

thesH143

Small scale interactions in the near sur



3 2768 002 13681 4

DUDLEY KNOX LIBRARY